ACS chemical biology

Letters

pubs.acs.org/acschemicalbiology

Protein Recognition by Short Peptide Reversible Inhibitors of the Chromatin-Modifying LSD1/CoREST Lysine Demethylase

Marcello Tortorici,[†,#] Maria Teresa Borrello,[‡,#] Maria Tardugno,[‡,§,#] Laurent R. Chiarelli,[†] Simona Pilotto,[†] Giuseppe Ciossani,[†] Nadeem A. Vellore,[∥] Sarah G. Bailey,[⊥] Jonathan Cowan,[‡] Maria O'Connell,[‡] Simon J. Crabb,[⊥] Graham Packham,[⊥] Antonello Mai,[§] Riccardo Baron,*[,∥] A. Ganesan,*[,‡] and Andrea Mattevi*[,†]

[†]Department of Biology and Biotechnology, University of Pavia, via Ferrata 9, 27100 Pavia, Italy

[‡]School of Pharmacy, University of East Anglia, Norwich Research Park, Norwich NR47TJ, United Kingdom

[§]Department of Drug Chemistry and Technologies, University "La Sapienza", P. le A. Moro 5, Roma 00185, Italy

[∥]Department of Medicinal Chemistry, College of Pharmacy, and The Henry Eyring Center for Theoretical Chemistry, The University of Utah, Salt Lake City, Utah 84112-5820, United States

[⊥]Cancer Research UK Centre, University of Southampton, Faculty of Medicine, Southampton General Hospital, Tremona Road, Southampton SO16 6YD, United Kingdom

Supporting Information

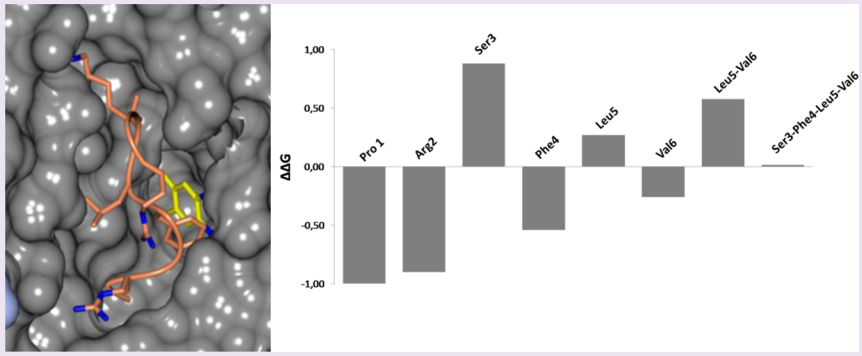

ABSTRACT: The combinatorial assembly of protein complexes is at the heart of chromatin biology. Lysine demethylase LSD1(KDM1A)/CoREST beautifully exemplifies this concept. The active site of the enzyme tightly associates to the N-terminal domain of transcription factors of the SNAIL1 family, which therefore can competitively inhibit the binding of the N-terminal tail of the histone substrate. Our enzymatic, crystallographic, spectroscopic, and computational studies reveal that LSD1/CoREST can bind to a hexapeptide derived from the SNAIL sequence through recognition of a positively charged α-helical turn that forms upon binding to the enzyme. Variations in sequence and length of this six amino acid ligand modulate affinities enabling the same binding site to differentially interact with proteins that exert distinct biological functions. The discovered short peptide inhibitors exhibit antiproliferative activities and lay the foundation for the development of peptidomimetic small molecule inhibitors of LSD1.

Histone-modifying and chromatin-binding proteins bind in a specific manner to amino acid sequences of different lengths that are often, but not always, located in the N-terminal region of histone proteins. An excellent example is given by the lysine specific demethylase LSD1 (KDM1A).[1,2] In association with the corepressor CoREST, this flavoenzyme is an 'eraser' that selectively demethylates Lys4me/me2 of histone H3. However, this enzymatic activity is modulated by the presence or absence of other H3 post-translational modifications. Furthermore, at least the first 21 N-terminal amino acids of the H3 tail are necessary for significant substrate recognition by the enzyme[2] (see Table 1 for K_i values).

LSD1 is widely investigated for its expanding biological roles and involvement in cancer, neurodegeneration, and viral infection.[3,4] The enzyme is homologous to monoamine oxidases (MAOs), and anti-MAO drugs are being preclinically investigated as demethylase inhibitors. There remains the issue of selectivity and the fact that these compounds are covalent modifiers of the FAD cofactor,[5] while the reported reversible LSD1 inhibitors are modest in activity or polycationic in nature.[6,7] Here, we show the first short peptides (MW < 800)

Received: March 21, 2013
Accepted: May 30, 2013
Published: May 30, 2013

Table 1. K_i Values for LSD1/CoREST Inhibition

peptide	sequence[a]	K_i (μM)[c]
H3 1−21[b]	ARTKQTARKSTGGKAPRKQLA	1.8 ± 0.6
H3 1−12[b]	ARTKQTARKSTG	199.0 ± 22.0
H3 6−21[b]	TARKSTGGKAPRKQLA	87.0 ± 29.0
SNAIL1 1−20	PRSFLVRKPSDPNRKPNYSE	0.21 ± 0.07
INSM1 1−20	PRGFLVKRSKKSTPVSYRVR	0.24 ± 0.10
SNAIL1 1−9	PRSFLVRKP	0.14 ± 0.06
SNAIL1 1−6	PRSFLV	28.4 ± 4.8
SNAIL1 1−5	PRSFL	120 ± 20
SNAIL1 1−4	PRSF	>1000
SNAIL1 2−6	RSFLV	451 ± 89
SNAIL1 1−6	PRSFLV-OH	60.2 ± 12.7

[a]Except for the last entry, all peptides in this and subsequent tables are C-terminal amides. [b]Data are from refs 2 and 12. [c]In all cases, peptides exhibited competitive inhibition (see Methods section).

that inhibit LSD1 in a reversible manner, opening new avenues for inhibitor design and drug discovery. Variations in the sequence and length of these minimal peptides modulate binding affinities and elucidate the ability of the LSD1 active site cleft to distinguish between histone substrates and other binding partners.

An unusual aspect of LSD1 biology was unveiled by the discovery that SNAIL1 exerts a repressive activity by recruiting and directing LSD1 to target genes.[8] SNAIL1 is a member of the SNAIL/SCRATCH family of transcription factors that are involved in a variety of cell differentiation and development processes.[9] We have shown that the N-terminal 21 amino acids of SNAIL1 (the 'SNAG' domain) binds to the LSD1 active site in a conformation similar to that of H3. Thus, SNAIL1 competes with the H3 substrate and effectively functions as an endogenous inhibitor of LSD1.[10] While LSD1 binding to the H3 substrate involves multiple interactions and at least the first 16 residues, the X-ray analysis of the complex of LSD1/CoREST with the SNAIL1 N-terminal peptide showed that only the first 9 amino acids have well-defined electron density. This suggests that residues 10−21 might be disordered or bound with multiple conformations (Figures 1 and S1, Supporting Information). To verify this crucial point, we studied a 20-mer peptide corresponding to the sequence of INSM1, another member of the SNAIL/SCRATCH family. Compared to SNAIL1, this protein differs by a Ser to Gly substitution at position 3 and a totally different sequence after residue 8 (Table 1). We found that INSM1 binds to LSD1/CoREST with the same affinity as SNAIL1 as measured by

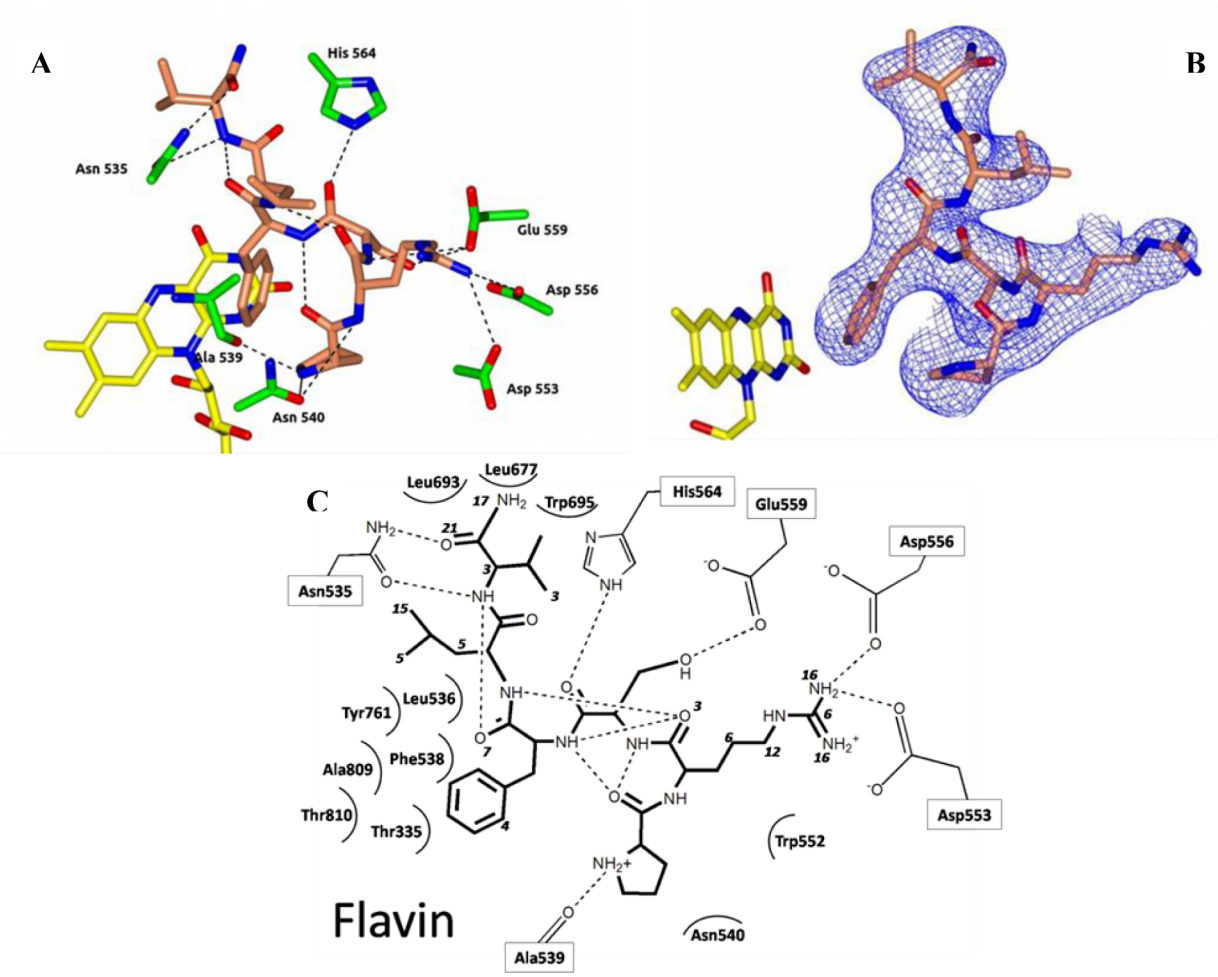

Figure 1. (a) Three-dimensional view of PRSFLV (the N-terminal hexapeptide of human SNAIL1) binding in the LSD1 active site. Protein carbons are shown in green, FAD carbons in yellow, and peptide carbons in brown. H-bonds are shown as dashed lines. (b) The unbiased 2Fo−Fc electron density map (contoured at the 1.2σ level) calculated prior to inclusion of the peptide in the refinement. (c) Schematic representation of the peptide−protein interactions. The atomic accessible surface areas (when ≥3 Å^2) are shown.

dx.doi.org/10.1021/cb4001926 | ACS Chem. Biol. 2013, 8, 1677−1682

enzymatic assays. Furthermore, the crystal structure indicated that only residues 1−8 bind with an ordered conformation that is virtually indistinguishable from that exhibited by SNAIL1 (Figures S1 and S2, Supporting Information). This initial observation led us to investigate truncated SNAG domains in search of the minimal requirement for binding. We discovered that the first six amino acid residues of SNAIL1 are sufficient to bind LSD1/CoREST with low micromolar affinity. Although longer peptides such as the nonamer have stronger affinity for LSD1, their ligand efficiency is poorer compared to this lower molecular weight hexamer, which we selected for further optimization.

Having discovered the minimal hexapeptide PRSFLV, we made a series of substitutions to identify the residues important for interactions with the core of the LSD1 cleft (Table 2).

Table 2. SAR Studies on the Hexapeptide PRSFLV with Altered Residues Indicated in Bold and K_i Values for Binding to LSD1/CoREST

sequence	K_i (μM)
Ala Scanning	
PRSFLV	28.4 ± 4.8
ARSFLV	157.8 ± 16.5
PA**S**FLV	130.0 ± 50.0
PR**A**FLV	6.4 ± 1.3
PRS**A**LV	71.4 ± 15.1
PRSF**A**V	18.0 ± 5.4
PRSFL**A**	44.4 ± 5.4
Side Chain Mutations	
LRSFLV	171.9 ± 12.5
P**L**SFLV	55.0 ± 11.00
P**K**SFLV	49.6 ± 8.23
PRS**Y**LV	25.0 ± 3.00
PRS**W**LV	118.7 ± 18.30
PRS**R**LV	58.0 ± 11.00
PRS**M**LV	2.6 ± 0.66
PRS**Kme$_2$**LV[a]	19.7 ± 2.30
PR**L**YLV	29.1 ± 3.90
PRSF**AA**	10.7 ± 1.1
PR**AAAA**	27.7 ± 4.0
SNAIL1-H3 Hybrid	
PRSF**QTV**	8.0 ± 1.9

[a]Considering that Phe4 of SNAIL1 corresponds to Lys4 of H3 (i.e., the site of demethylation), it is of notice that the peptide with dimethylLys4 is an inhibitor rather than a substrate, implying that the context of the H3 sequence is essential for the catalytically competent positioning of the reactive methyl-Lys group.

Above all, deletion or Ala and Leu substitutions of Pro1 turned out to be very detrimental to binding. Proline is a known helix breaker, but it also has some propensity to function as the N-capping amino acid of α-helices.[11] In the case of LSD1, Pro1 can initiate the helical turn of the bound peptide and be buried in the hydrophobic niche of the cleft that hosts the N-terminal residue of the peptide (Figures 1 and S3, Supporting Information). The next residue Arg2 also significantly contributes to binding since mutations to Lys, Leu, and, to a bigger extent, Ala all decrease affinity. This side chain extensively interacts with a ring of Asp and Glu side chains at the rim of the cleft, and its aliphatic portion is involved in intrapeptide contacts with Leu5, which might favor the helical conformation (Figures 1 and S3, Supporting Information). By contrast, the residues 3−6 have more ancillary roles because mutations generally do not affect binding affinities and conformations (Figure S1, Supporting Information). The only exceptions are the Trp and Met replacements of Phe4. The bulky indole ring of Trp causes a 4-fold increase of the K_i, whereas the presence of Met generates a high-affinity peptide (K_i of 3 μM), similarly to the enhanced affinity exhibited by the H3 peptide bearing the Lys4Met substitution.[12] Thus, the hydrophobic Met side chain is able to establish favorable interactions with the flavin cofactor promoting tight binding. Conclusive support to the notion that side chains 3−6 are not essential for binding was given by two peptides with multiple Ala residues (PRSFAA and PRAAAA), as they bind with affinities identical to that of the native SNAIL1 sequence. Overall, our data suggests that the active site of LSD1 is suited to host short peptides beginning with the Pro1−Arg2 sequence (Figure S3, Supporting Information).

Our analysis of seven crystal structures of LSD1/CoREST bound to SNAIL-derived peptides indicated that, in all cases, the N-terminal residues bind to the enzyme cleft in a helical conformation (Figure S1 and Table S1, Supporting Information). Prompted by this observation, we sought to gain further insight into whether the peptides exist in folded conformations or are largely unfolded and disordered in solution and fold only upon binding to the enzyme. To probe the peptide conformation in solution, we carried out circular dichroism spectroscopy on four peptides (H3 21-mer, INSM1 20-mer, SNAIL1 20-mer, and SNAIL1 9-mer; Figure 2). We found that the spectrum of the SNAIL1 9-mer was very different from that predicted for the conformation of the peptide bound to LSD1/CoREST. Furthermore, none of the tested peptides exhibited the spectroscopic properties expected for α-helical or β-strand conformations, indicating that the unbound peptides mostly exist as random conformers. This notion was further corroborated by computational studies. We performed 150 ns of molecular dynamic simulations using AMBER program with explicit solvent[13] as well as Replica Exchange MD simulations for 50 ns[14,15] to investigate the native structure of H3, SNAIL1, and INSM1 10-mer and 20-mer peptides in solution. None of the sequences exhibited marked folding preferences. Only a few transient secondary structures were observed during the course of the simulation with residues 1−4 having a small propensity for α-helix (about 7%), whereas residues 5−8 were partly involved in a β-turn (H3 < 10%; INSM1 and SNAIL1 = 35%). Collectively, the studies suggest that the peptides exist as random conformers and form the secondary structure only upon LSD1 binding.

The active site cleft of LSD1 can bind to its histone H3 substrate at variable affinities by sensing the presence or absence of epigenetic marks on the histone tail, and it is able to tightly interact with the N-terminal residues of the SNAIL family of transcription factors that have only limited homology to the H3 sequence. In relation to SNAIL1 binding, the N-terminal Pro1 residue is particularly crucial since its replacement with Ala and Leu drastically decreases affinity. As H3 instead contains an N-terminal Ala1, this change can largely explain the poor binding of short H3 peptides to LSD1. To test this hypothesis, we prepared a hybrid peptide with SNAIL1 1−4 grafted onto H3 5−7 and indeed found that it binds with significant affinity (Table 2). A second aspect is that residues 10−20 of SNAIL1 peptides do not contribute to binding (Table 1). This is entirely consistent with the sequence homology because SNAIL1 transcription factors are highly

dx.doi.org/10.1021/cb4001926 | ACS Chem. Biol. 2013, 8, 1677−1682

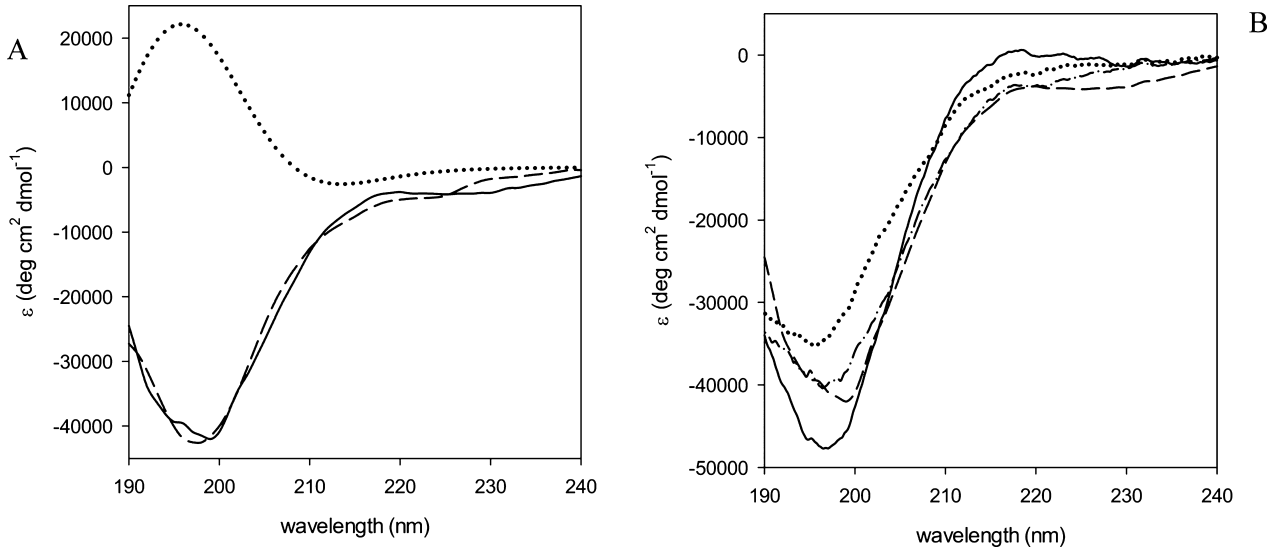

Figure 2. Far-UV circular dichroism spectra. (a) Comparison of the experimental spectrum of SNAIL1 peptide (1−9; —) with that calculated from the conformation of the same peptide bound to LSD1/CoREST (●●●●●; PDB entry 2Y48) and the theoretical spectrum of a random coil (− −). (b) Spectra of H3 (residues 1−21; —), INSM1 (1−20; ●●●●●), SNAIL1 (1−20; − ● −), and SNAIL1 (1−9; − −) peptides in solution. In all cases, spectral curves correspond closely to those expected for >90% random coil conformation.

conserved in their first nine N-terminal residues, whereas their sequences diverge after this initial strictly conserved segment.[9] This is not the case for the H3 N-terminal tail, whose binding can take place (though weakly) also for peptides that lack the first five N-terminal amino acids and substantially depends also on residues after Arg8 (Table 1). Thus, on one hand, the presence of Ala1 (instead of Pro1) diminishes the contribution to binding of the very first N-terminal stretch of the H3 peptide, but on the other hand, this is partly compensated by the contribution given by the more distant residues in positions 10−20 along the H3 sequence. Indeed, the crystal structure shows that the H3 residues 9−16 are engaged in a network of intra- and intermolecular H-bond interactions, which critically depend on the amino acid sequence.[12] Our observations are of particular interest as a starting point for the development of noncovalent selective inhibitors of LSD1 with potential as anticancer agents.[4] A SNAG domain linked to the Tat cell penetrating tag was shown to block the repression of the E-cadherin promoter.[16] Although our short peptides do not contain a cell penetrating tag, they nevertheless mirror the biological properties displayed by covalent LSD inhibitors. The peptides act as inhibitors of proliferation in leukemia cell lines, and their effect on LSD1 is confirmed by a significant increase in the H3-Lys4 methylation levels (at 1 mM concentrations; Figure S4, Supporting Information). Therefore, the discovery of small LSD1/CoREST peptide ligands lays the foundation for the structure-based development of further analogues with improved drug-like properties. The added value of these compounds is that they can function as inhibitors of both the enzymatic activity as well as the interactions with transcription factors controlling cell differentiation processes.

METHODS

Inhibition Assays. Peptide syntheses are described in the Supporting Information. A His-tagged recombinant form of human LSD1 comprising residues 171−836 was copurified with a GST-tagged CoREST protein (residues 308−440) by tandem-affinity chromatography followed by gel filtration on a Superdex200 column (GE Healthcare).[12] Peptide inhibition was evaluated by a coupled enzymatic assay monitoring hydrogen peroxide formation.[12] The reaction mixture contained 50 mM Hepes pH 7.5, 0.1 mM 4-aminoantipyrine, 1 mM 3,5-dichloro-2-hydroxybenzenesulfonic acid, 2.8 μM horseradish peroxidase, 1 μM LSD1/CoREST, and varying peptide ligands (0−50 μM) and dimethylated H3−K4 peptide substrate (2−30 μM) concentrations. Absorbance changes were monitored at 515 nm (ε_{515} = 26 000 M^{-1} cm^{-1}) at 25 °C using a Cary 100 spectrophotometer. Initial velocity values were fitted to equations describing competitive, uncompetitive, and noncompetitive inhibition patterns using Grafit (Erithacus Software) to obtain the values for the kinetic parameters along with their associated errors. In all cases, the best fit was obtained with the equation describing a competitive inhibition.

X-ray crystallography. The LSD1/CoREST complex was crystallized at 20 °C as described.[12] Peptide complexes were obtained by crystals soaking in solutions consisting of 1.6 M sodium/potassium tartrate, 100 mM *N*-(2-acetamido)-2-iminodiacetic acid pH 6.5, 10% (v/v) glycerol, and 2−5 mM peptide for 3 h. X-ray diffraction data were collected at 100 K at beamlines of the Swiss Light Source (Villigen, Switzerland) and ESRF (Grenoble, France). Data processing and crystallographic refinement were carried out using programs of the CCP4 package[17] (Figure S1 and Table S1, Supporting Information).

Computational Analysis. Peptides were modeled using the tLEAP program to represent an apparent neutral pH[18] and solvated using a pre-equilibrated box of TIP3P water molecules, maintaining a minimum distance of 10 Å between any peptide atom and the box edges.[19] Their initial configurations were generated by setting all dihedral angles to trans configuration. Periodic boundary conditions were imposed using a truncated octahedron box. Cl^- ions were added to neutralize the systems using previously proposed AMBER-compatible ion parameters.[20] The total number of atoms, water molecules, and ions in the simulated systems are as follows: 10-mers, H3, 9436 atoms, 3087 water molecules, and 4 Cl^- ions; SNAIL1, 9160 atoms, 2993 water molecules, and 3 Cl^- ions; INSM-10mer, 10 209 atoms, 3341 water molecules, and 4 Cl^- ions. 20-mers, H3, 36 341 atoms, 11 999 water molecules, and 7 Cl^- ions; SNAIL1, 36 339 atoms, 11 999 water molecules, and 3 Cl^- ions; INSM, 36 368 atoms, 12 002 water molecules, and 7 Cl^- ions. All systems were energy minimized using 1000 steps of steepest descent and 1000 steps of conjugate gradient standard procedures. MD simulations were carried out in three phases for heat-up, equilibration, and production. During the heat-up phase, the peptide positions were restrained using a weak harmonic potential with a force constant of 10 kcal/mol/Å^2. A two-

dx.doi.org/10.1021/cb4001926 | *ACS Chem. Biol.* 2013, 8, 1677−1682

step equilibration was performed using 1 ns of NVT ensemble followed by 5 ns of constant 1 atm pressure simulation. During the equilibration run, all the bonds involving hydrogen atoms were restrained using the SHAKE algorithm,[21] thus allowing a 2 fs time step for integration of Newton's equations. All the systems were simulated for additional 150 ns production runs in the NPT ensemble using the GPU version of the AMBER12 program.[22] In all cases, a Langevin dynamics integrator with a collision frequency (γ) of 2 ps^{-1} was employed, and the Particle Mesh Ewald approximation was used for full electrostatic interactions (real space interactions truncated at 10 Å).[23] Replica Exchange MD (REMD) simulations[14] were performed on the same systems with a total of 32 (10-mer) or 72 (20-mer) replicas, and an exponential temperature distribution from 300 to 450 K. Exchanges were attempted for every 1 ps and a total of 50 ns was generated for each system. The baseline temperature (300 K) was utilized for analyzing the secondary structures of the peptide using the PTRAJ module of AmberTools. The PMEMD routine of AMBER12 was used for REMD simulations. Snapshots from MD and REMD simulations were extracted every 1 ps for analysis.

Circular Dichroism. Spectra were measured at RT with a Jasco J-710 spectropolarimeter using peptide concentrations of 20−120 μM in 2 mM potassium phosphate pH 7.5, 0.5% (v/v) glycerol. Data were analyzed with DichroWeb and DichroCalc.[24,25]

Antiproliferation Assay and Western Blotting. HL-60 cells were cultured in RPMI 1640 medium with 10% (v/v) fetal calf serum (FCS), 2 mM L-glutamine, and penicillin/streptomycin (100 U/mL and 100 μg/mL, respectively). Cells were maintained at 37 °C in an atmosphere of 5% CO_2. Antiproliferation assay was carried out using MTS reagent (CellTiter96 Aqueous One Solution Cell Proliferation Assay). Cells were plated in a 96-well plate at a concentration of 5×10^4 cells/well and 3×10^4 cells/well, respectively, and immediately treated with 1 μL of peptide diluted in PBS (phosphate buffered saline-peptide vehicle) at different concentrations (2 mM, 1 mM, 500 μM, 250 μM, 125 μM, 62 μM, 31 μM, and 15 μM). After 72 h of incubation, 10 μL of prewarmed MTS reagent was added to each well, and after 3 h, the absorbance was measured at 492 nm on a BMG PolaSTAR OPTIMA plate reader (BMG Labtech). Experiments were performed in triplicate. Data were analyzed using Graphpad prism to calculate standard error of the mean. For the Western blots (Figure S4, Supporting Information), HL-60 cells were treated for 4 h with 1 mM of tranylcypromine (Sigma-Aldrich, Poole, UK) or 1 mM peptides. Whole cell lysates were then analyzed by Western blot (Abcam antibodies) for H3K4me2 levels with total H3 as the loading control.

■ ASSOCIATED CONTENT

Ⓢ Supporting Information

Additional methods and supporting figures and tables. This material is available free of charge via the Internet at http://pubs.acs.org.

Accession Codes

Coordinates and structure factors have been deposited with the PDB (3zms, 3zmt, 3zmu, 3zmv, 3zmz, 3zn0, 3zn1; see also Table S1, Supporting Information).

■ AUTHOR INFORMATION

Corresponding Author

*(A.M.) E-mail: andrea.mattevi@unipv.it. Tel: +39-0382-985534. (A.G.) E-mail: a.ganesan@uea.ac.uk. Tel: +44(0) 1603597154. (R.B.) E-mail: r.baron@utah.edu. Tel: +1-801-585-7117.

Author Contributions

#These authors contributed equally to this work.

Notes

The authors declare no competing financial interest.

■ ACKNOWLEDGMENTS

We thank the Department of Medicinal Chemistry at the University of Utah, Fondazione Cariplo (2010.0778), Associazione Italiana Ricerca sul Cancro (IG-11342), MIUR (Epigen), the University of East Anglia, and the COST Action TD0905 Epigenetics: Bench to Bedside for financial support. R.B. acknowledges a generous allocation at XSEDE (TG-CHE120086; supported by NSF grant OCI-1053575).

■ REFERENCES

(1) Shi, Y., Lan, F., Matson, C., Mulligan, P., Whetstine, J. R., Cole, P. A., Casero, R. A., and Shi, Y. (2004) Histone demethylation mediated by the nuclear amine oxidase homolog LSD1. *Cell 119*, 941−953.

(2) Forneris, F., Binda, C., Battaglioli, E., and Mattevi, A. (2008) LSD1: oxidative chemistry for multifaceted functions in chromatin regulation. *Trends Biochem. Sci. 33*, 181−189.

(3) Schenk, T., Chen, W. C., Göllner, S., Howell, L., Jin, L., Hebestreit, K., Klein, H. U., Popescu, A. C., Burnett, A., Mills, K., Casero, R. A., Jr., Marton, L., Woster, P., Minden, M. D., Dugas, M., Wang, J. C., Dick, J. E., Müller-Tidow, C., Petrie, K., and Zelent, A. (2012) Inhibition of the LSD1 (KDM1A) demethylase reactivates the all-trans-retinoic acid differentiation pathway in acute myeloid leukemia. *Nat. Med. 18*, 605−611.

(4) Black, J. C., Van Rechem, C., and Whetstine, J. R. (2012) Histone lysine methylation dynamics: Establishment, regulation, and biological impact. *Mol. Cell 48*, 491−507.

(5) Benelkebir, H., Hodgkinson, C., Duriez, P. J., Hayden, A., Bullied, R., Crabb, S. J., Packham, G., and Ganesan, A. (2011) Enantioselective synthesis of tranylcypromine analogues as lysine demethylase (LSD1) inhibitors. *Bioorg. Med. Chem. 19*, 3709−3716.

(6) Wang, J., Lu, F., Ren, Q., Sun, H., Xu, Z., Lan, R., Liu, Y., Ward, D., Quan, J., Ye, T., and Zhang, H. (2011) Novel histone demethylase LSD1 inhibitors selectively target cancer cells with pluripotent stem cell properties. *Cancer Res. 71*, 7238−7249.

(7) Willmann, D., Lim, S., Wetzel, S., Metzger, E., Jandausch, A., Wilk, W., Jung, M., Forne, I., Imhof, A., Janzer, A., Kirfel, J., Waldmann, H., Schule, R., and Buettner, R. (2012) Impairment of prostate cancer cell growth by a selective and reversible lysine-specific demethylase 1 inhibitor. *Int. J. Cancer 131*, 2704−2709.

(8) Lin, Y., Wu, Y., Li, J., Dong, C., Ye, X., Chi, Y. I., Evers, B. M., and Zhou, B. P. (2010) The SNAG domain of Snail1 functions as a molecular hook for recruiting lysine-specific demethylase 1. *EMBO J. 29*, 1803−1816.

(9) Barrallo-Gimeno, A., and Nieto, M. A. (2009) Evolutionary history of the Snail/Scratch superfamily. *Trends Genet. 25*, 248−252.

(10) Baron, R., Binda, C., Tortorici, M., McCammon, J. A., and Mattevi, A. (2011) Molecular mimicry and ligand recognition in binding and catalysis by the histone demethylase LSD1-CoREST complex. *Structure 19*, 212−220.

(11) Kim, M. K., and Kang, Y. K. (1999) Positional preference of proline in alpha-helices. *Protein Sci. 8*, 1492−1499.

(12) Forneris, F., Binda, C., Adamo, A., Battaglioli, E., and Mattevi, A. (2007) Structural basis of LSD1-CoREST selectivity in histone H3 recognition. *J. Biol. Chem. 282*, 20070−20074.

(13) Hornak, V., Abel, R., Okur, A., Strockbine, B., Roitberg, A., and Simmerling, C. (2006) Comparison of multiple Amber force fields and development of improved protein backbone parameters. *Proteins 65*, 712−725.

(14) Okamoto, Y. S. Y. (1999) Replica-exchange molecular dynamics method for protein folding. *Chem. Phys. Lett. 314*, 141−151.

(15) Pitera, J. W., and Swope, W. (2003) Understanding folding and design: replica-exchange simulations of "Trp-cage" miniproteins. *Proc. Natl. Acad. Sci. U.S.A. 100*, 7587−7592.

(16) Ferrari-Amorotti, G., Fragliasso, V., Esteki, R., Prudente, Z., Soliera, A. R., Cattelani, S., Manzotti, G., Grisendi, G., Dominici, M., Pieraccioli, M., Raschellà, G., Claudia, C., Colombo, M. P., and Calabretta, B. (2012) Inhibiting interactions of lysine demethylase

LSD1 with Snail/Slug blocks cancer cell invasion. *Cancer Res. 73*, 235−245.
(17) Winn, M. D., Ballard, C. C., Cowtan, K. D., Dodson, E. J., Emsley, P., Evans, P. R., Keegan, R. M., Krissinel, E. B., Leslie, A. G., McCoy, A., McNicholas, S. J., Murshudov, G. N., Pannu, N. S., Potterton, E. A., Powell, H. R., Read, R. J., Vagin, A., and Wilson, K. S. (2011) Overview of the CCP4 suite and current developments. *Acta Crystallogr., Sect. D: Biol. Crystallogr. 67*, 235−242.
(18) Case, D. A.; Darden, T. E.; Cheatham, C. L.; Simmerling, J.; Wang, R. E.; Duke, R. *AMBER12*, 2012.
(19) Jorgensen, W. L., Chandrasekhar, J., Madura, J. D., Impey, R. W., and Klein, M. L. (1983) Comparison of simple potential functions for simulating liquid water. *J. Chem. Phys. 79*, 926−931.
(20) Joung, I. S., and Cheatham, T. E., III. (2008) Determination of alkali and halide monovalent ion parameters for use in explicitly solvated biomolecular simulations. *J. Phys. Chem. B 112*, 9020−9041.
(21) Miyamoto, S., and Settle, P. A. K. (1992) An analytical version of the SHAKE and RATTLE algorithm for rigid water models. *J. Comput. Chem. 13*, 952−962.
(22) Gotz, A. W., Williamson, M. J., Xu, D., Poole, D., Le Grand, S., and Walker, R. C. (2012) Routine microsecond molecular dynamics simulations with AMBER on GPUs. 1. Generalized Born. *J. Chem. Theory Comput. 8*, 1542−1555.
(23) Darden, T., York, D., and Pedersen, L. (1993) Particle mesh Ewald: An N-log(N) method for Ewald sums in large systems. *J. Chem. Phys. 98*, 10089−10093.
(24) Whitmore, L., and Wallace, B. A. (2008) Protein secondary structure analyses from circular dichroism spectroscopy: methods and reference databases. *Biopolymers 89*, 392−400.
(25) Bulheller, B. M., and Hirst, J. D. (2009) DichroCalc: Circular and linear dichroism online. *Bioinformatics 25*, 539−540.